Numerical Computation of Fluid Flow and Aerosol Particle Transport In A Long Electrical Mobility Spectrometer

ORIGINALITY REPORT

8%	8%	0%	%
SIMILARITY INDEX	INTERNET SOURCES	PUBLICATIONS	STUDENT PAPERS

MATCH ALL SOURCES (ONLY SELECTED SOURCE PRINTED)

8%

★ repositori.ukdc.ac.id

Internet Source

Exclude quotes	Off	Exclude matches	< 2%
Exclude bibliography	On		

Numerical Computation of Fluid Flow and Aerosol Particle Transport In A Long Electrical Mobility Spectrometer

by Lasman Parulian Purba

Submission date: 04-Sep-2021 10:16AM (UTC+0700)
Submission ID: 1641165920
File name: cle,_Numerical_Simulation,_Electrical_Mobility,_Spectrometer.pdf (3.92M)
Word count: 2336
Character count: 11926

TSF

ME-NETT23

The 23rd Conference of the Mechanical Engineering Network of Thailand
November 4 – 7, 2009, Chiang Mai

Numerical Computation of Fluid Flow and Aerosol Particle Transport in a Long Electrical Mobility Spectrometer

Panich Intra[1]*, Lasman P. Purba[2] and Nakorn Tippayawong[3]

[1] College of Integrated Science and Technology, Rajamangala University of Technology Lanna, Chiang Mai, Thailand 50300
[2] Department of Mechanical Engineering, Prince of Songkla University, Hat Yai Campus, Thailand 90110
[3] Department of Mechanical Engineering, Chiang Mai University, Chiang Mai, Thailand 50200
*Corresponding Author: Tel. (668) 3921444 Ext. 1012, Fax: (665) 3213183,
E-mail: panich_intra@yahoo.com

Abstract

In this study, a numerical computational model for prediction of fluid flow and aerosol particle transport in a long column electrical mobility spectrometer (EMS) has been developed. The internal three-dimensional (3D) structure of an EMS (Intra and Tippayawong, *Korean J. Chem. Eng.*, 26(1), 269 (2009)) was employed to simulate the complex flow patterns and aerosol particle trajectories in the EMS, including the swirling flow that develops near the sheath air inlet slit. The incompressible Navier-Stokes equation is numerically calculated for the gas flow and particle trajectories, with a commercial computational fluid dynamics (CFD) software package, FLUENT 6.3, using a finite volume method. The calculated results agreed with the previous published results in the literature. Prediction of fluid flow and aerosol particle transport were also particularly useful in the EMS design.

Keywords: Aerosol, Particle, Numerical Simulation, Electrical Mobility, Spectrometer

1. Introduction

A long column electrical mobility spectrometer (EMS) is one of the most commonly used instruments for the measurement of aerosol particle size distribution in the nanometer-sized range based on their electrical mobility technique. The most widely used EMS is based on the design developed by Mirme [1]. Intra and Tippayawong [2] offers reviews of the recent development of this technique.

A typical setup of a general EMS consists of two concentric electrodes between which a potential is applied. There are two streams; polydisperse aerosol and sheath air flows. The inner electrode of the spectrometer is maintained at a DC high voltage while the outer chassis of the spectrometer is grounded. The charged particles enter the spectrometer column close to the inner electrode by a continuous flow of air, and surrounded by a sheath air flow. Since the

inner electrode is kept at a high voltage, the charged particles are deflected outward radially. They are collected on a series of electrically isolated electrometer rings positioned at the inner surface of the outer chassis of the spectrometer column. Virtual ground potential input of highly sensitive electrometers are connected to these electrometer rings to measure currents corresponding to the number concentration of particles in a given mobility which is in turn related to the particle size distribution. Resolution of the instrument is determined mainly by the number and width of the electrometer rings. The size range of particle collected on the electrometer rings can be varied by adjusting the aerosol and sheath air flow rates, the voltage applied to the inner electrode, and the operating pressure.

It is well known that fluid flow and particle transport inside the EMS are important factor influencing accurate particle size distribution measurements. Fluid flow and particle transport inside the EMS has recently been studied by many people [3 – 8]. To our knowledge, the issue of a 3D simulation of fluid flow and particle transport in the long EMS has not been extensively studied in literature. In this paper, a 3D computational model for prediction of fluid flow and aerosol particle transport inside a long EMS developed at Chiang Mai University was developed and studied. A detailed description of the operating principle of the EMS is also presented.

2. Description of a Long EMS

The EMS has one long column, consisting of coaxially cylindrical electrodes. Fig. 1 shows a schematic diagram of the long EMS used in this study [9]. Outer chassis is made of a 481 mm long aluminum tube with an internal diameter of 55 mm. Inner electrode is made of a 25 mm in diameter stainless steel rod. Width of the aerosol inlet channel is 2 mm. The sheath-air flow entered with a swirl component and then flowed through a 0.1 mm thick Teflon mesh to ensure the flow was laminar. The 22 electrometer rings used result in the classification of every measured aerosol into 22 mobility ranges. The electrometer rings have a width of 19 mm. The first electrometer ring is located 20 mm downstream the aerosol inlet, while a 1 mm gap is allowed between the electrometer rings for electrical isolation.

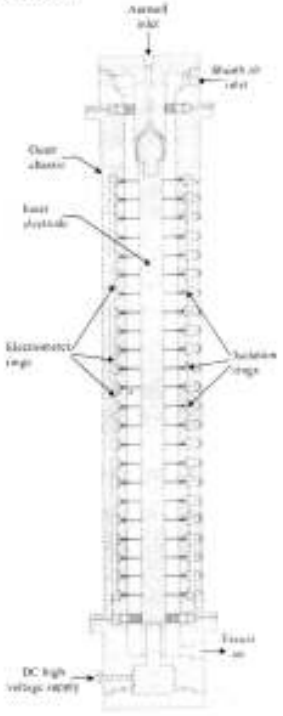

Fig. 1 Schematic diagram of the long EMS [1]

3. Physical Modelling

Gas flow and particles motion are numerically modeled and solved to estimate the particle transport in an EMS.

3.1 Gas continuity

The gas flow is considered the main phase and its motion is described by the continuity and the momentum equations, known as the Navier-Stokes equations

$$\frac{\partial}{\partial x_i}(\rho u_i) = 0 \qquad (1)$$

where ρ is the gas density, and u_i is the gas velocity component in the x_i direction.

3.2 Gas momentum

$$\frac{\partial}{\partial x_i}\left(\rho u_i u_i - (\mu + \mu_t)\frac{\partial u_i}{\partial x_i}\right) = -\frac{\partial p}{\partial x_i} + f_D \qquad (2)$$

where ρ is the mass density of the gas, u is the gas velocity, μ is the gas molecular dynamic viscosity, f_D is the aerodynamic drag force, and p is the gas pressure.

3.3 Particles motion

Aerosol particles are accelerated by the aerodynamic drag. When collision and coagulation between particles can be neglected, the equation of the particle motion is expressed as:

$$\frac{dx_i}{dt} = v_i \qquad (3)$$

$$m_p \frac{dv_i}{dt} = \frac{1}{C_c} 3\pi\mu d_p (u_i - v_i) \qquad (4)$$

where m_p is the particle mass, v_i is the particle velocity, C_c is the Cunningham correction factor, and d_p is the particle diameter.

4. Computational Modelling

4.1 Method of solution

Fluid flow and particle trajectories in an internal 3D structure of an EMS are calculated by the commercial CFD package, FLUENT 6.3, using a finite volume method for the incompressible Navier-Stokes equation in 3D cylindrical coordinates. The solution domain is divided into a number of cells known as control volumes. In the finite volume approach of FLUENT 6.3, the governing equations for the gas flow and the particles motion are numerically integrated over each of these computational cells or control volumes.

4.2 Boundary conditions

The computational domain of the EMS is shown in Fig. 2. The model EMS consists of the aerosol and sheath air inlets, and outlet boundaries. As shown in the Fig. 2, no slip boundary is applied to all the solid walls included in the computation domain and fixed velocity boundary conditions were applied to the aerosol and sheath air flow inlets. The velocities at each inlet were calculated from the flow rates through these slits. Uniform velocity profile is assumed at the sheath and aerosol inlet across the cross section of the inlet tubes. Boundary conditions used in this calculation are summaries in Table 1.

4.3 Computational mesh

Fig. 3 shows a computational mesh used for the fluid flow and particle transport simulations. Finer grids are used in the region close to the aerosol entrance and where the velocity gradient is expected to be large. An unstructured mesh is used. A total of about 869,401 meshes are distributed in computational domain of internal flows in the EMS.

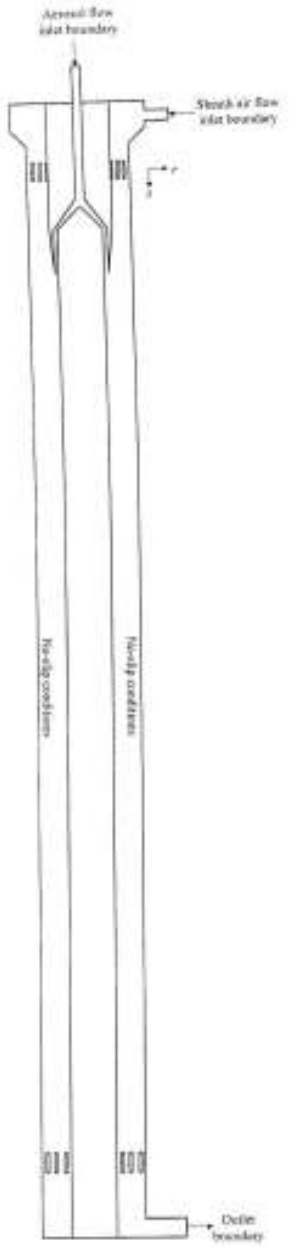

Fig. 2 Computational domain of the EMS

Table 1 Boundary conditions for numerical calculation

Air velocity at aerosol inlet	u_x = 0.0 m/s
	u_y = 0.0 m/s
	u_z = 0.106 m/s
Air velocity at sheath air inlet	u_x = 7.43 m/s
	u_y = 0.0 m/s
	u_z = 0.0 m/s
Air velocity at outlet	mass conservation
Inner electrode	no slip
Electrometer rings	no slip
Insulator rings	no slip

(a) Total view

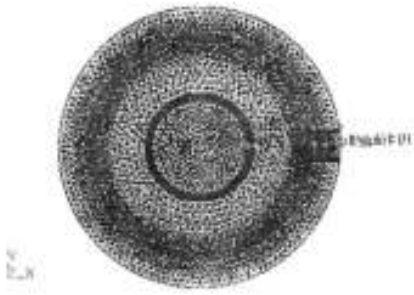

(b) Cross section view

Fig. 3 Computational mesh of the EMS

5. Results and Discussion

The operating gas was ambient air (density is 1.225 kg/m^3 and viscosity is 1.7894 x 10^{-5} kg/m/s), while particle diameter is 10 – 1000 nm. Fig. 4 shows the CFD calculations of the fluid flow velocity in the EMS. The high towards low intensity regions were indicated by red, yellow, green to blue, respectively. Fig. 4(b) shows the detailed flow matching condition around the aerosol and sheath air inlets. Nonuniform flow velocity distribution was found near the aerosol and sheath air inlet boundaries. In general, the flow profile becomes fully developed at a few hydraulic diameters downstream from the aerosol inlet, while negligible disturbances occur at the point where the two flows (aerosol and sheath air) merge. Fig. 4(c) shows the detailed flow velocity around the excess air outlet. It can be seen that the highest flow velocity was found in the excess air outlet, located in the bottom left corner side of the model. Flow simulation results showed similar trend to those by the previous published results in the literature [3 – 8].

Fig. 5 shows CFD calculation results of the massless particle trajectories inside the EMS. The massless particles enter from aerosol and sheath air inlets to excess air outlet. Fig. 5(b) and 5(c) shows trajectories of massless particles around the aerosol and sheath air inlet, and excess air outlet. The uniform distribution of particles was found at downstream from the aerosol and sheath air inlet. It was also shown that the nonuniformity of particle circumferential distribution that exists near the aerosol and sheath air inlets and excess air outlet is caused by a nonuniform gas velocity distribution in the vicinity of the aerosol and sheath air inlets.

(a) Total view

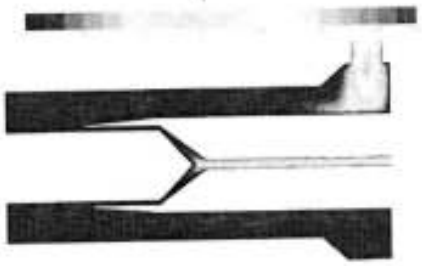

(b) The regions close to aerosol and sheath air inlets

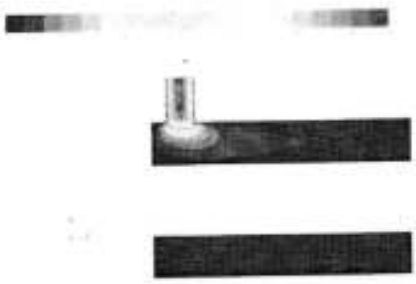

(c) The regions close to excess air outlet

Fig. 4 CFD calculations of the fluid flow velocity inside the EMS

(a) Total view

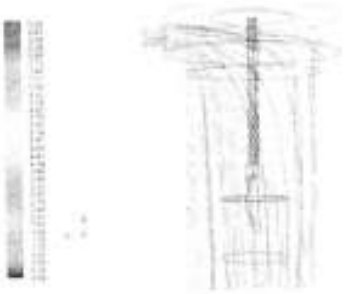

(b) The regions close to aerosol and sheath air inlets

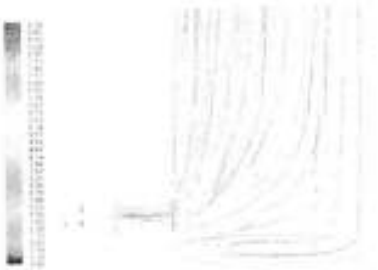

(c) The regions close to excess air outlet

Fig. 5 CFD calculations of the massless particle trajectories inside the EMS

With regards to sizing ultrafine aerosol particles of diameter smaller than a few tens of nm, Brownian diffusion motion becomes important [9]. Since the aerosol is entered into the EMS column through a narrow annular slit, the EMS transmission efficiency drops significantly for particles below 10 nm due to diffusion losses in the annulus and other flow passages. Further, long residence time in the EMS column region results in substantial Brownian diffusion broadening of the transfer function for nanometer-sized particles. Fig. 6 shows particle trajectories in the EMS with taking into account the Brownian diffusion effect for particle diameters of 10, 100, and 1000 nm. It was shown that smaller particles were found to exhibit higher Brownian diffusive motion than the larger particles. It is apparent that Brownian diffusion significantly affects particle trajectories when the diameter is smaller than 10 nm [9, 10]. CFD results also showed similar with the previous work [9].

6. Conclusions

A 3D numerical model was developed for the description of fluid flow and aerosol particle transport inside the long EMS. The model was developed with the commercial CFD package, FLUENT 6.3. The model was extensively applied to 3D geometry provided with detail: (a) the gas flow field and (b) particle trajectories. It was shown that the numerical simulation results exhibited a qualitatively well-agreed trend with the published results in the literature. It has been demonstrated here that a numerical model can be used to predict flow field and particle transport, hence, assist in designing an EMS for nanometer-sized aerosol particle measurement. For future study, an experimental validation is also planned.

(a) 10 nm

(b) 100 nm

(c) 1000 nm

Fig. 6 CFD calculations of the particle trajectories inside the EMS

7. Acknowledgement

The authors wish to express their deepest gratitude to the National Electronic and Computer Technology Center, Thailand for their financial support of this project, contract no. NT-B-22-SS-11-50-18.

8. References

[1] Mirme, A. (1994). Electric Aerosol Spectrometry, Ph.D. Thesis, University of Tartuensis, Tartu, Estonia.

[2] Intra, P. and Tippayawong, N. (2008). An overview of differential mobility analyzers for size classification of nanometer-sized aerosol particles, *Songklanakarin Journal of Science and Technology*, vol.30(2), pp. 243 – 256.

[3] Chen, D. R. and Pui, D.Y.H. (1997). Numerical modeling of the performance of differential mobility analyzer for nanometer aerosol measurements, *Journal of Aerosol Science*, vol.28(6), pp. 985 – 1004.

[4] Otani, Y., Emi, H., Cho, S. and Okuyama, K. (1997). Technique for aerosol flow check in differential mobility analyzer and its influence on classification performance, *Journal of Chemical Engineering of Japan*, vol.30(6), pp. 1065 – 1069.

[5] Chen, D. R., Pui, D.Y.H., Hummes, D., Fissan, H., Quant, F. R. and Sem, G. J. (1998). Design and evaluation of a nanometer aerosol differential mobility analyzer (nano-DMA), *Journal of Aerosol Science*, vol.29(5/6), pp. 497 – 509.

[6] Chen, D. R., Pui, D.Y.H., Mulholland, G. W. and Fernandez, M. (1999). Design and testing of an aerosol/sheath inlet for high resolution measurements with a DMA, *Journal of Aerosol Science*, vol.30(8), pp. 983 – 999.

[7] Asai, T., Shimada, M., Okuyama, K., Kim, T. and Komatsubara, M. (1999). Numerical